Geology

Controls on fluvial evacuation of sediment from earthquake-triggered landslides

--Manuscript Draft--

Manuscript Number:	G36157R1
Full Title:	Controls on fluvial evacuation of sediment from earthquake-triggered landslides
Short Title:	fluvial residence time of coseismic landslide
Article Type:	Article
Keywords:	Wenchuan earthquake; residence time; landslide; suspended sediment
Corresponding Author:	Zhangdong Jin Institute of Earth Environment, Chinese Academy of Sciences Xi'an, Shaanxi CHINA
Corresponding Author Secondary Information:	
Corresponding Author's Institution:	Institute of Earth Environment, Chinese Academy of Sciences
Corresponding Author's Secondary Institution:	
First Author:	Jin Wang
First Author Secondary Information:	
Order of Authors:	Jin Wang
	Zhangdong Jin
	Robert Hilton
	Fei Zhang
	Alexander Densmore
	Gen Li
	A. Joshua West
Order of Authors Secondary Information:	
Manuscript Region of Origin:	CHINA
Abstract:	Large earthquakes in active mountain belts can trigger landslides which mobilize large volumes of clastic sediment. Delivery of this material to river channels may result in aggradation and flooding, while sediment residing on hillslopes may increase the likelihood of subsequent landslides and debris flows. Despite this recognition, the controls on the residence time of coseismic landslide sediment in river catchments remain poorly understood. Here we assess the residence time of fine-grained (<0.25 mm) landslide sediment mobilized by the 2008 Mw 7.9 Wenchuan earthquake, China, using daily suspended sediment discharge measured in 16 river catchments from 2006 to 2012. Following the earthquake, suspended sediment discharge was elevated 3-7 times compared to 2006-2007. However, the total 2008-2012 export (92.5 ± 9.3 Mt from 68,719 km2) was much less than estimates of fine-grained sediment input by coseismic landslides (418+437/-302 Mt) determined by landslide area-volume scaling and deposit grain-size distributions. We estimate the residence time of fine-grained sediment in the affected river catchments using the post-earthquake rate of sediment export, and find it ranges from one year to over a century. The first-order variability in fine sediment residence time is proportional to the areal extent of coseismic landsliding, and is inversely proportional to the frequency of intense runoff events (>5 mm day-1). Together with previous observations from the 1999 Chi-Chi earthquake in Taiwan, our results demonstrate the importance of landslide density and runoff intensity in setting the duration of earthquake-triggered landslide impacts on river systems.
Response to Reviewers:	

Publisher: GSA
Journal: GEOL: Geology
DOI:10.1130/G36157.1

Controls on fluvial evacuation of sediment from earthquake-triggered landslides

Jin Wang[1,2,3], Zhangdong Jin[1,4]*, Robert G. Hilton[2], Fei Zhang[1], Alexander L. Densmore[2,5], Gen Li[6], and A. Joshua West[6]

[1]*State Key Laboratory of Loess and Quaternary Geology, Institute of Earth Environment, Chinese Academy of Sciences, Xi'an 710075, China*

[2]*Department of Geography, Durham University, Durham, DH1 3LE, UK*

[3]*University of Chinese Academy of Sciences, Beijing 100049, China*

[4]*Institute of Global Environmental Change, Xi'an Jiaotong University, Xi'an 710049, China*

[5]*Institute of Hazard, Risk and Resilience, Durham University, Durham, DH1 3LE, UK*

[6]*Department of Earth Sciences, University of Southern California, Los Angeles, California 90089, USA*

*E-mail address: zhdjin@ieecas.cn

ABSTRACT

Large earthquakes in active mountain belts can trigger landslides which mobilize large volumes of clastic sediment. Delivery of this material to river channels may result in aggradation and flooding, while sediment residing on hillslopes may increase the likelihood of subsequent landslides and debris flows. Despite this recognition, the controls on the residence time of coseismic landslide sediment in river catchments remain poorly understood. Here we assess the residence time of fine-grained (<0.25 mm) landslide sediment mobilized by the 2008 M_w 7.9

Wenchuan earthquake, China, using daily suspended sediment discharge measured in 16 river catchments from 2006 to 2012. Following the earthquake, suspended sediment discharge was elevated 3–7 times compared to 2006-2007. However, the total 2008-2012 export (92.5 ± 9.3 Mt from 68,719 km^2) was much less than estimates of fine-grained sediment input by coseismic landslides (418+437/-302 Mt) determined by landslide area-volume scaling and deposit grain-size distributions. We estimate the residence time of fine-grained sediment in the affected river catchments using the post-earthquake rate of sediment export, and find it ranges from one year to over a century. The first-order variability in fine sediment residence time is proportional to the areal extent of coseismic landsliding, and is inversely proportional to the frequency of intense runoff events (>5 mm day^{-1}). Together with previous observations from the 1999 Chi-Chi earthquake in Taiwan, our results demonstrate the importance of landslide density and runoff intensity in setting the duration of earthquake-triggered landslide impacts on river systems.

INTRODUCTION

Large earthquakes can trigger widespread coseismic landslides which mobilize large volumes of sediment (Keefer, 1984; 1994). Landslide sediment can cause river bed aggradation, increasing the frequency and magnitude of floods (e.g. Korup et al., 2004) and affect water resources and hydro-electric power generation (Glade and Crozier, 2005). Export of sediment mobilized by coseismic landslides also governs the role of earthquakes in landscape evolution (Hovius et al., 2011; Li et al., 2014). Despite this recognition, the timescales over which earthquake-landslide sediment impacts river catchments remain poorly constrained. Examples from Papua New Guinea, New Zealand and Japan have provided estimates of the time required to remove coseismic landslide sediment from catchments, termed here the ‘residence time’, that range from <1 year to >50 years (Pain and Bowler, 1973; Pearce and Watson, 1986; Koi et al., 2008; Howarth et al., 2012). In Taiwan, intense precipitation associated with tropical cyclones after the 1999 M_w 7.6 Chi-Chi earthquake led to greatly enhanced sediment export and the return of suspended sediment loads to pre-earthquake levels within ~6 years (Dadson et al., 2004; Yanites et al., 2010; Hovius et al., 2011; Huang and Montgomery, 2012). However, we lack a holistic view of what controls the residence time of earthquake-mobilized sediment across events and river catchments, necessary to better manage earthquake hazards (Keefer, 1994; Huang and Fan, 2013) and to understand landscape evolution (Li et al., 2014).

Here we examine the impact of the 2008 M_w 7.9 Wenchuan earthquake, which triggered more than 57,150 landslides in the Longmen Shan, China (Li et al., 2014), on three major river catchments (Min Jiang, Tuo Jiang, and Fu Jiang) (Fig. 1). The earthquake provides insight due to: i) the large spatial gradients in coseismic landsliding (Li et al., 2014) and ii) the variable climate and therefore the variable sediment transport conditions across the impacted area (Liu-Zeng et al., 2011). These factors allow us to assess the relative importance of sediment supply and fluvial transport capacity in setting the residence time of earthquake-mobilized sediment. The Wenchuan earthquake occurred along the Beichuan and Pengguan faults at the eastern margin of the Tibetan Plateau (Xu et al., 2009), where the regional climate is dominated by the East Asian and Indian summer monsoons. Annual precipitation is 600–1,100 mm yr^{-1}, with 70–80% of rainfall between

May and October (Liu-Zeng et al., 2011). Coseismic landslides mobilized ~2.8+0.9/-0.7 km^3 of clastic sediment in the three major river basins (Li et al., 2014). Using a data set of unprecedented temporal resolution, we examine the immediate (daily to weekly) and longer-term (years to decades) impacts of earthquake-triggered landslides on river suspended loads and assess the controls on fine-grained sediment residence time.

MATERIALS AND METHODS

Daily water discharge (Q_w, $m^3\ s^{-1}$) and daily suspended sediment concentration (SSC, mg L^{-1}) were measured at 16 gauging stations of the Chinese Bureau of Hydrology from 2006 to 2012 (Table DR1 in the GSA Data Repository[1]). Ten stations are located downstream of heavily landslide-impacted areas (Li et al., 2014), where landslide areal density ρ_{ls} (the fraction of area affected by landslide scars) reach > 1%. Six stations have lower ρ_{ls} (Fig. 1). SSC samples were collected up to 8 times per day, depending upon water level variations, with a depth-integrated sampler along 5–10 vertical profiles (Ministry of Water Resources of China, 2007). Samples were filtered through 0.7 µm paper filters, and the sediment was dried and weighed. The grain size distribution was measured on selected samples. Daily suspended sediment discharge (SSC × Q_w) was summed to quantify annual suspended sediment discharge, Q_{ss} (Mt yr^{-1}). Uncertainties on SSC were estimated using the standard deviation of daily repeat SSC measurements at the Sangping station and were propagated into estimates of Q_{ss} (Table DR2). Before and after the earthquake, 97% of suspended sediment was transported between May and October during monsoonal rainfall (Fig. DR1). During winter, some rivers have very low Q_w and SSC, so 10 of 16 stations only measured SSC from April or May to October. Only measured samples were used to quantify annual suspended discharge.

Estimates of landslide sediment volume (V_{ls}, m^3) in each catchment were taken from Li et al. (2014), who mapped the areas (A_{ls}, m^2) of coseismic landslides. Total V_{ls} was estimated using a power law relationship between A_{ls} and V_{ls} (Guzzetti et al., 2009; Larsen et al., 2010), with a coefficient (α) and exponent (γ) derived from field measurements of 41 landslides within the Longmen Shan (Parker et al., 2011; Li et al., 2014). The uncertainties on the total volume of the 57,150 landslides were determined by Monte Carlo simulation taking errors on α and γ into account (Li et al., 2014). To compare landslide inputs to suspended load Q_{ss}, we used a compilation of grain size measurements from 33 sites across 9 landslide deposits in the major river basins (Table DR3). Across these sites, the average weight percent of material <0.25 mm in diameter was 6.6 ± 4.4% (±1σ), which we use to estimate fine sediment volume and its likely variability in the landscape.

FLUVIAL RESPONSE TO THE WENCHUAN EARTHQUAKE

The three major rivers draining the impacted area experienced an increase in Q_{ss} following the earthquake (Fig. 1). At the most downstream gauging stations, post-earthquake Q_{ss} was ~3 to ~7 times higher than in 2006-2007 (Fig. 1). These increases are similar to those in Taiwan rivers impacted by the 1999 Chi-Chi earthquake (Dadson et al., 2004; Hovius et al., 2011). In contrast to the elevated post-earthquake Q_{ss} values (Fig. 1), changes in annual water discharge were relatively minor (Fig. DR2). The enhanced Q_{ss} is consistent with observations of dilution of ^{10}Be concentrations in detrital quartz in some of the studied catchments (West et al., 2014). Input of ^{10}Be-depleted landslide material is thought to be responsible for a decrease in detrital ^{10}Be of river sediments (0.25-1 mm) and suggest that sediment discharge increased ~2 to ~9 times in the 2 years following the earthquake (West et al., 2014).

The daily measurements also reveal the immediate fluvial response to the earthquake and its aftershocks. At Sangping station on the Zagunao River (drainage area 4,600 km^2, ρ_{ls} ~0.3%; Table DR1), SSC 18 h after the earthquake (1,532 mg L^{-1}) was 57 times higher than that measured 6 h before the earthquake (27 mg L^{-1}), while Q_w remained roughly constant (Fig. 2A). This immediate response is consistent with delivery of some fine-grained coseismic landslide sediment directly to rivers. SSC then decreased over ~10 days while Q_w was relatively invariant, indicating removal of available sediment from the banks and bed of the active river channel (Fig. 2A).

Three measurements depart significantly from this pattern (Fig. 2A). First, higher SSC values on 14/05/2008 (1,756 mg L^{-1}) and 15/05/2008 (2,652 mg L^{-1}) were measured within 24 h of the first large aftershock occurred within 20 km of the gauging station (M_w 5.4, 10:54 on 14/05/2008; USGS, 2013). Then, SSC doubled (from 796 to 1,347 mg L^{-1}) between 08:00 and 20:00 on 16/05/2008, coincident with an M_w 5.6 aftershock (13:26 on 16/05/2008; USGS, 2013) which occurred 26 km from the station. We tentatively link these aftershocks to the further supply of fine-grained sediment to the river channel, through either new landslides or remobilization of loose material.

The Q_{ss} at Sangping over the 10 days following the earthquake (Fig. 2A) was 0.09 ± 0.02 Mt, much less than the estimated fine-grained landslide inputs of 10+12/-8 Mt upstream of the station. Therefore, to elucidate the longer-term pattern of sediment export, we use two sets of nested gauging stations upstream and downstream of the landslide-affected area (Fig. 1). To average over short-term variability (e.g. Fig. 2A), we sum Q_{ss} over half-year time intervals and calculate the 'downstream sediment gain', the ratio of downstream to upstream Q_{ss}. After the earthquake, downstream sediment gain increased by ~4 times in the Zagunao River along a 55 km reach with ρ_{ls} ~0.3% (Fig. 2B), and increased by ~12 times in the Fu Jiang along a 105 km reach with ρ_{ls} ~0.6% (Fig. 2C). In both locations, downstream water gain showed no change after the earthquake (Fig. DR3).

Post-earthquake decline in the downstream sediment gain for the Fu Jiang can be described by a power-law function of time (r^2 = 0.94) (Fig. 2C). This declining trend suggests that the suspended sediment loads would return to pre-earthquake levels in 6 ± 1 years, similar to estimates following the Chi-Chi earthquake in Taiwan (Hovius et al., 2011). In contrast, in the Zagunao River the post-earthquake decline in downstream sediment gain within the 4 years of our data set is less clear (Fig. 2B). In this case, a power-law curve does not describe the trend well (r^2 = 0.39), and the data suggest that elevated suspended load may persist for longer than in the Fu Jiang. To better understand the fluvial response to the earthquake, we examine all catchments in the Longmen Shan and consider both the coseismic landslide sediment input and the climatic setting of each basin.

RESIDENCE TIME OF EARTHQUAKE-MOBILIZED SEDIMENT

Over the Longmen Shan, the mean annual Q_{ss} following the earthquake (2008–2012) was 18.5 ± 7.4 Mt yr^{-1} (±1σ). Deducting an estimate of the background Q_{ss} (2006–2007, 4.2 ± 2.6 Mt yr^{-1}), the excess Q_{ss} attributable to the earthquake was 14.3 ± 7.8 Mt yr^{-1} (Table DR1). Most (>95%) of this mass is fine sediment, <0.25 mm (Fig. DR4). In contrast, 2.4+1.9/-0.7 km^3 of sediment was mobilized by earthquake-triggered landslides (Li et al., 2014), equating to 6329+5097/-1787 Mt (assuming a solid density of 2.65×10^3 kg m^{-3}). Of this sediment, available data suggests that 6.6 ± 4.4% has a grain size of <0.25 mm (Table DR3). Acknowledging the uncertainty on these estimates, we estimate a total supply of fine (<0.25 mm) landslide sediment of 418+437/-302 Mt.

Across the Longmen Shan, at the present rate of post-earthquake fluvial export, we estimate that it will take 29+30/-21 years to remove all material <0.25 mm delivered by coseismic landslides (Table DR1). This estimate does not consider a decline in Q_{ss} over time (Fig. 2C) and so provides a lower bound on residence time. Estimates of fine sediment residence time in individual catchments range from 1.0+1.6/-0.9 to 77+109/-65 yr, with an extreme value of 190+528/-186 yr (Table DR1). The residence time estimated from Fujiangqiao station (5+8/-4 yr) is consistent with the estimate made from the decline of sediment load in this catchment of 6 ± 1 yr (Fig. 2C).

CONTROLS ON SEDIMENT RESIDENCE TIME

The estimated residence times of fine-grained coseismic landslide sediment in the Longmen Shan span the range estimated from previous earthquakes (Pain and Bowler, 1973;

Pearce and Watson, 1986; Koi et al., 2008, Hovius et al., 2011; Howarth et al., 2012). Here we assess the controls on this variability. For a given catchment hydrological regime and transport capacity, an increase in sediment supply should increase the residence time of that sediment (Pearce and Watson, 1986; Benda and Dunne, 1997; Yanites et al., 2010). The data from the Longmen Shan are broadly consistent with this hypothesis: catchments with low coseismic landslide density (ρ_{ls} < 0.2%) generally have shorter fine sediment residence times than those with ρ_{ls} > 0.6% (Fig. 3), assuming that V_{ls} scales with A_{ls}. However, this only partly explains the variability between catchments.

In the Longmen Shan, the contribution of intense runoff events (daily Q_w normalized by catchment area) varies between catchments (Fig. DR5). The proportion of total catchment runoff delivered by daily flows >5 mm day^{-1} varies from 0 to 66% across the study area (Table DR1). For a given landslide density, a higher proportion of intense runoff leads to a shorter fine sediment residence time (Fig. 3), likely due to a combination of increased river transport capacity and enhanced mobilization of sediment from existing deposits (Benda and Dunne, 1997; Dadson et al., 2004). In addition, heavy rainfall can trigger landslides on earthquake-weakened slopes (Dadson et al., 2004). The very long fine residence time in Santai (187+510/-153 yr) is more than double any other catchment and cannot be well explained by runoff intensity and ρ_{ls} alone. There, the very long residence time may reflect large individual landslides that contribute significant volumes of sediment but limited total landslide area (Fig. DR6). The additional variability (Fig. 3) may be due to secondary factors (e.g. spatial variability in landslide connectivity, channel order, channel

DOI:10.1130/G36157.1

gradients, channel length, and anthropogenic activities) which can moderate Q_{ss} (Benda and Dunne, 1997). The scatter also reflects the uncertainty in the quantification of residence time, derived mainly from uncertainty in the volume of fine sediment from landslides and its grain size. Nevertheless, our data suggest that runoff intensity plays a crucial role in regulating the residence time of fine sediment mobilized by a major earthquake (Fig. 3).

WIDER IMPLICATIONS

Our analysis can explain the relatively short residence time of fine sediment after the 1999 M_w 7.6 Chi-Chi earthquake in Taiwan (Hovius et al., 2011) as compared with the range of responses in the Longmen Shan catchments (Fig. 3). In Taiwan, 11 large tropical cyclones in 1999-2007 each delivered the annual runoff of the Longmen Shan (~0.4–0.7 m, ~1–2 km^3 of water) over a period of 10–30 days (Hovius et al., 2011). This intense runoff delivery is reflected in the Chenyoulan catchment, where ~60% of the annual runoff is delivered by events with >5 mm day^{-1}, higher than any catchment impacted by Wenchuan earthquake (Figs. 3 and DR5). These cyclones triggered additional post-seismic landslides (Dadson et al., 2004). Despite this additional sediment input, suspended sediment loads returned to pre-earthquake levels in ~6 yr. The short-lived fluvial influence of Chi-Chi landslide sediment can thus be attributed to intense precipitation during tropical cyclones, which enables the rapid erosion, transport and export of landslide-mobilized sediment. These observations are also consistent with lake records of fine sediment accumulation driven by earthquakes on the Alpine Fault, New Zealand. There, enhanced sediment export from catchments appears to last for ~50 yr following earthquakes (Howarth et al., 2012). While total runoff is high in the western Southern Alps, it is delivered at a lower intensity than in Taiwan (Dadson et al., 2004; Hovius et al., 2011).

Our results suggest that the combination of coseismic landslide density and the frequency of intense runoff events appears to govern, to first order, the residence time of fine-grained sediment (Fig. 3). This may also be the case for coarser sediment, but it is not straightforward to extend our analysis to coarse-grained landslide material transported as bed load (Pearce and Watson, 1986; Korup et al., 2004) which can reside in catchments for much longer periods of time (Benda and Dunne, 1997; Yanites et al., 2010; Huang and Montgomery, 2012). Nevertheless, river catchments with high coseismic landslide density and infrequent high runoff events may have long memories of large earthquakes (Fig. 3), posing a significant challenge to hazard management (Huang and Fan, 2013).

ACKNOWLEDGMENTS

This research was funded by the 973 program (2013CB956402) to Z.J., NSFC grants and CAS YIS Fellowships to A.J.W. and R.G.H., a U.S. NSF Grant (EAR/GLD 1053504) to A.J.W., and a Royal Society Grant (RG110569) to R.G.H. We thank Y. Peng, F. Li, and Q. Zhang for assistance in the data collection and A. Galy, P. Molnar, R. Parker and J. Yu for discussions during manuscript preparation. J. Spotila, D. Lague, I. Larsen and three anonymous referees are thanked for their insightful comments which improved the manuscript.

REFERENCES CITED

Benda, L., and Dunne, T., 1997, Stochastic forcing of sediment supply to channel networks from landsliding and debris flow: Water Resources Research, v. 33, p. 2849–2863, doi:10.1029/97WR02388.

Dadson, S.J., Hovius, N., Chen, H., Dade, W.B., Lin, J.-C., Hsu, M.-L., Lin, C.-W., Horng, M.-J., Chen, T.-C., Milliman, J., and Stark, C.P., 2004, Earthquake-triggered increase in sediment delivery from an active mountain belt: Geology, v. 32, p. 733–736, doi:10.1130/G20639.1.

Glade, T., and Crozier, M.J., 2005, The nature of landslide hazard impact, *in* Glade, T., Anderson, M., and Crozier, M.J., eds., Landslide Hazard and Risk: Chichester, John Wiley & Sons, Ltd, p. 41–74.

Guzzetti, F., Ardizzone, F., Cardinali, M., Rossi, M., and Valigi, D., 2009, Landslide volumes and landslide mobilization rates in Umbria, central Italy: Earth and Planetary Science Letters, v. 279, p. 222–229, doi:10.1016/j.epsl.2009.01.005.

Hovius, N., Meunier, P., Lin, C.-W., Chen, H., Chen, Y.-G., Dadson, S., Horng, M.-J., and Lines, M., 2011, Prolonged seismically induced erosion and the mass balance of a large earthquake: Earth and Planetary Science Letters, v. 304, p. 347–355, doi:10.1016/j.epsl.2011.02.005.

Howarth, J.D., Fitzsimons, S.J., Norris, R.J., and Jacobsen, G.E., 2012, Lake sediments record cycles of sediment flux driven by large earthquakes on the Alpine fault, New Zealand: Geology, v. 40, p. 1091-1094, doi:10.1130/G33486.1.

Huang, M.Y.-F., and Montgomery, D.R., 2012, Fluvial response to rapid episodic erosion by earthquake and typhoons, Tachia River, central Taiwan: Geomorphology, v. 175–176, p. 126-138, doi:10.1016/j.geomorph.2012.07.004.

Huang, R., and Fan, X., 2013, The landslide story: Nature Geoscience, v. 6, p. 325–326, doi:10.1038/ngeo1806.

Keefer, D.K., 1984, Landslides caused by earthquakes: Geological Society of America Bulletin, v. 95, p. 406–421, doi:10.1130/0016-7606(1984)95<406:LCBE>2.0.CO;2.

Keefer, D.K., 1994, The importance of earthquake-induced landslides to long-term slope erosion and slope-failure hazards in seismically active regions: Geomorphology, v. 10, p. 265–284, doi:10.1016/0169-555X(94)90021-3.

Koi, T., Hotta, N., Ishigaki, I., Matuzaki, N., Uchiyama, Y., and Suzuki, M., 2008, Prolonged impact of earthquake-induced landslides on sediment yield in a mountain watershed: The Tanzawa region, Japan: Geomorphology, v. 101, p. 692–702, doi:10.1016/j.geomorph.2008.03.007.

Korup, O., McSaveney, M.J., and Davies, T.R.H., 2004, Sediment generation and delivery from large historic landslides in the Southern Alps, New Zealand: Geomorphology, v. 61, p. 189–207, doi:10.1016/j.geomorph.2004.01.001.

Larsen, I.J., Montgomery, D.R., and Korup, O., 2010, Landslide erosion controlled by hillslope material: Nature Geoscience, v. 3, p. 247–251, doi:10.1038/ngeo776.

Publisher: GSA
Journal: GEOL: Geology
DOI:10.1130/G36157.1

Li, G., West, A.J., Densmore, A.L., Jin, Z., Parker, R.N., and Hilton, R.G., 2014, Seismic mountain building: Landslides associated with the 2008 Wenchuan earthquake in the context of a generalized model for earthquake volume balance: Geochemistry Geophysics Geosystems, v. 15, p. 833–844, doi:10.1002/2013GC005067.

Liu-Zeng, J., Wen, L., Oskin, M., and Zeng, L., 2011, Focused modern denudation of the Longmen Shan margin, eastern Tibetan Plateau: Geochemistry Geophysics Geosystems, v. 12, Q11007, doi:10.1029/2011GC003652.

Ministry of Water Resources of China, 2007, Code for Measurements of Suspended Sediment in Open Channels (GB50159–92): Beijing, China Planning Press (in Chinese).

Pain, C., and Bowler, J., 1973, Denudation following the November 1970 earthquake at Madang, Papua New Guinea: Zeitschrift fur Geomorphologie, v. 18, supplement, p. 92–104.

Parker, R.N., Densmore, A.L., Rosser, N.J., de Michele, M., Li, Y., Huang, R., Whadcoat, S., and Petley, D.N., 2011, Mass wasting triggered by the 2008 Wenchuan earthquake is greater than orogenic growth: Nature Geoscience, v. 4, p. 449–452, doi:10.1038/ngeo1154.

Pearce, A.J., and Watson, A.J., 1986, Effects of earthquake-induced landslides on sediment budget and transport over a 50-yr period: Geology, v. 14, p. 52–55, doi:10.1130/0091-7613(1986)14<52:EOELOS>2.0.CO;2.

USGS, U.S. Geological Survey Earthquake Hazards Program: http://earthquake.usgs.gov/earthquakes/map/, (accessed August 2013).

West, A.J., Hetzel, R., Li, G., Jin, Z., Zhang, F., Hilton, R.G., and Densmore, A.L., 2014, Dilution of Be-10 in detrital quartz by earthquake-induced landslides: Implications for determining denudation rates and potential to provide insights into landslide sediment dynamics: Earth and Planetary Science Letters, v. 396, p. 143–153, doi:10.1016/j.epsl.2014.03.058.

Xu, X., Wen, X., Yu, G., Chen, G., Klinger, Y., Hubbard, J., and Shaw, J., 2009, Coseismic reverse- and oblique-slip surface faulting generated by the 2008 Mw 7.9 Wenchuan earthquake, China: Geology, v. 37, p. 515–518, doi:10.1130/G25462A.1.

Yanites, B.J., Tucker, G.E., Mueller, K.J., and Chen, Y.G., 2010, How rivers react to large earthquakes: Evidence from central Taiwan: Geology, v. 38, p. 639–642, doi:10.1130/G30883.1.

FIGURE CAPTIONS

Figure 1. Major rivers impacted by the 2008 M_w 7.9 Wenchuan earthquake in the Longmen Shan, China (Min Jiang, Fu Jiang, and Tuo Jiang). River gauging stations used in this study are shown as circles. Nested gauging stations shown in Figure 2B and 2C are highlighted in yellow. Catchment color reflects the ratio of mean annual suspended sediment discharge (Q_{ss}, Mt yr^{-1}) after the earthquake to that prior to the earthquake. Contours show landslide areal density ρ_{ls} (%) calculated as the proportion of total area mapped as landslides (Li et al., 2014). Columns show the background Q_{ss} (white) and post-earthquake Q_{ss} (red).

Figure 2. Fluvial response to the 2008 Wenchuan earthquake. **A.** Suspended sediment concentration (SSC) measurements from the Zagunao River (Sangping station) in May 2008

before (gray circles) and after (red circles) the earthquake (red dashed line) and those taken shortly after aftershocks (blue dashed lines) within ~20 km of the gauging station (blue circles). Solid red line (r^2 = 0.51) is linear least-square best fit to the SSC data from 13 to 22 May. Daily water discharge normalized to the 2006-2011 average (Q_w/Q_{mean}) is shown as thicker solid line (gray). **B.** Downstream sediment gain on the Zagunao River – the ratio of downstream (Sangping station) to upstream (Zagunao station) Q_{ss} (Fig. 1). **C.** Downstream sediment gain on the Fu Jiang – the ratio of downstream (Fujiangqiao) to upstream (Pingwu) Q_{ss}. The dashed line is the best-fit power-law fit with 95% confidence intervals shown by dotted lines. On all panels whiskers show uncertainties (1σ) if larger than the point size.

Figure 3. Estimates of fine (<0.25 mm) coseismic landslide sediment residence time in river catchments impacted by the Wenchuan earthquake (circles), plotted as a function of the proportion of catchment runoff delivered by intense flows (> 5 mm day^{-1}) from May 2008 to Dec 2012. Shading of points reflects the upstream landslide areal density (%). Whiskers show propagated uncertainties of residence time of fine grained sediment. Star indicates comparable estimate from the 1999 Chi-Chi earthquake, Taiwan (Hovius et al., 2011).

[1]GSA Data Repository item 2014xxx, Figures DR1-6, Tables DR1-3 and Supplementary Information, is available online at www.geosociety.org/pubs/ft2014.htm, or on request from editing@geosociety.org or Documents Secretary, GSA, P.O. Box 9140, Boulder, CO 80301, USA.

Figure 1

Click here to download Figure: Wang et al-Figure 1.pdf

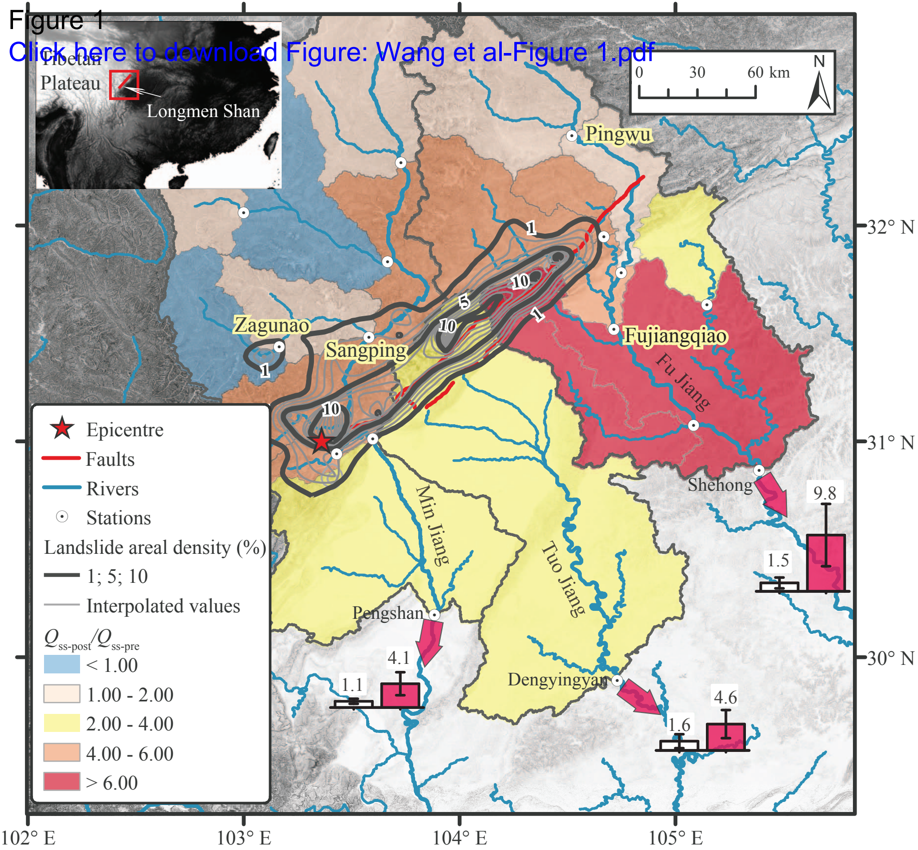

Figure 2

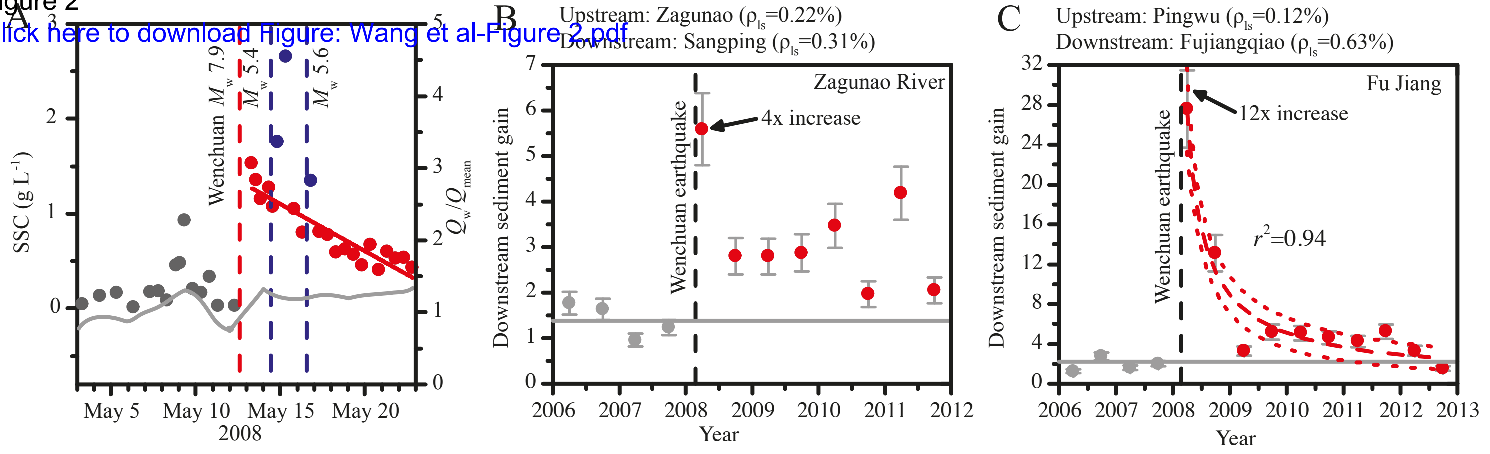
A
SSC (g L-1)
Q_w/Q_mean
Wenchuan M_w 7.9
M_w 5.4
M_w 5.6
May 5
May 10
May 15
May 20
2008
B
Upstream: Zagunao (ρ_ls=0.22%)
Downstream: Sangping (ρ_ls=0.31%)
Zagunao River
Wenchuan earthquake
4x increase
Downstream sediment gain
Year
C
Upstream: Pingwu (ρ_ls=0.12%)
Downstream: Fujiangqiao (ρ_ls=0.63%)
Fu Jiang
Wenchuan earthquake
12x increase
r2=0.94
Downstream sediment gain
Year

Figure 3

Click here to download Figure: Wang et al-Figure 3.pdf

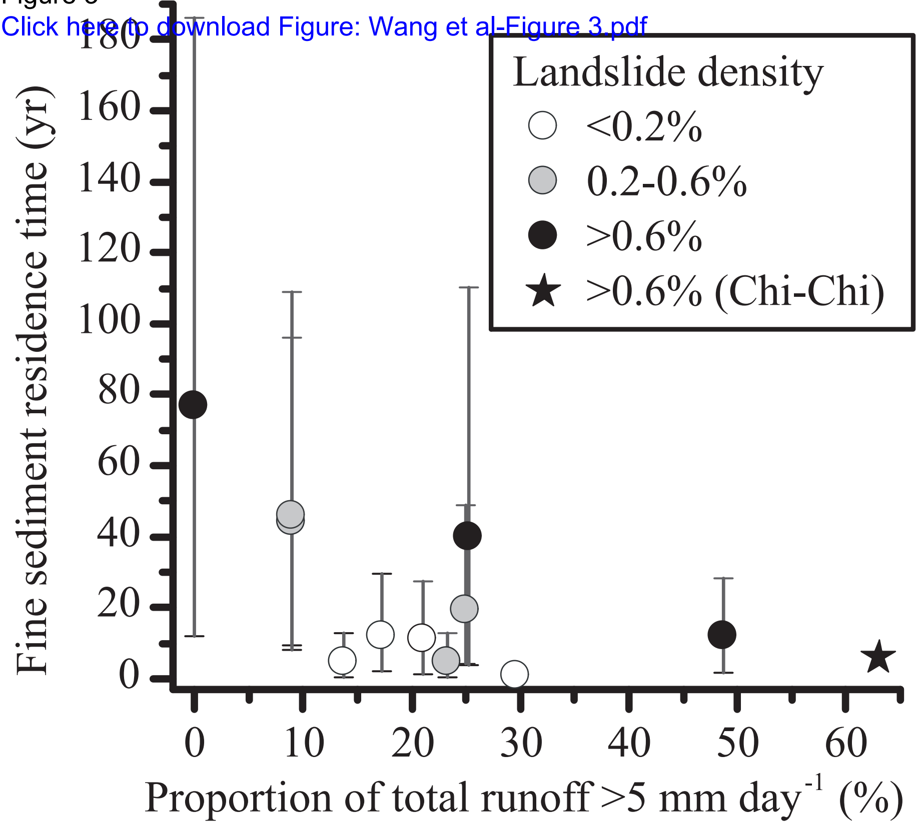

GSA DATA REPOSITORY

Controls on fluvial evacuation of sediment from earthquake-triggered landslides

Jin Wang[1,2,3], Zhangdong Jin[1,4]*, Robert G. Hilton[2], Fei Zhang[1], Alexander L. Densmore[2,5], Gen Li[6], and A. Joshua West[6]

[1] State Key Laboratory of Loess and Quaternary Geology, Institute of Earth Environment, Chinese Academy of Sciences, Xi'an 710075, China

[2] Department of Geography, Durham University, Durham, DH1 3LE, UK

[3] University of Chinese Academy of Sciences, Beijing 100049, China

[4] Institute of Global Environmental Change, Xi'an Jiaotong University, Xi'an 710049, China

[5] Institute of Hazard, Risk and Resilience, Durham University, Durham, DH1 3LE, UK

[6] Department of Earth Sciences, University of Southern California, Los Angeles, CA 90089, USA

Grain Size Distribution of Landslide Deposits

In this study, we use published measurements of the grain size distribution of landslide deposits formed during the 2008 Wenchuan earthquake (Table DR3) (Wang et al., 2011; Chen et al., 2012; Wang et al., 2012; Zhuang et al., 2012; Wang et al., 2013; Yu et al., 2013). Full details of methods can be found in these publications. Here, for summary, the procedure described by Wang et al. (2013) is provided. The grain size distribution of landslide sediment was analyzed by sieving and photography at 11 locations on the Tianchi landslide dam deposit. The area ratio of large grains with $\varphi > 40$ mm was measured by means of particle digital image analysis, using vertical photographs that were taken from a height of approximately 1.5 m above the ground surface. All visible individual grains >4.75 mm were outlined on the photographs, with the intermediate (b-axis) diameter and the cross-sectional area determined for each grain. For grains <4.75 mm, a 10 kg sample of ≤50 mm sediment was collected from each site and was sieved upon return to the laboratory. ASTM standards sieve series were utilized for this task. Assuming that the sediment has the same density, the weight percentages of grains with different grain sizes were calculated.

Grain Size Distribution of Suspended Sediments

The grain size distributions of suspended sediments were determined from samples collected from the three main rivers in the study area on the Min Jiang (Zhenjiangguan station), Tuo Jiang (Dengyingyan station) and Fu Jiang (Fujiangqiao station) (Fig. 1). The analyses were undertaken by the methods described in detail by

Guy (1969) and the Ministry of Water Resources of China (2005) and a summary is provided here. A depth-integrated and channel averaged suspended sediment sample was collected. Calgon solution was added to disperse and disaggregate clay particles and the sample was sieved at 0.063 mm. The >0.063 mm fraction was oven-dried at 100°C and the grain size distribution was determined by dry sieving at 2 mm, 1 mm, 0.5 mm, 0.25 mm and 0.125 mm. The <0.063 mm fraction was transferred to a 1 L graduated cylinder and was mixed for one minute until homogenized. Immediately after, 25 mL water was pipetted from the middle of cylinder to determine the total suspended load. Based on the predictable relationship between particle grain size and settling velocity in a fluid medium, the time and depth of subsequent pipette aliquots was determined on the basis of the Stokes law (e.g. for 25°C, time = 1’43”, D = 0.031 mm; time = 6’26”, D = 0.016 mm; time = 25’45”, D = 0.008 mm; time = 1h 43’, D = 0.004 mm). The pipetted samples were dried and weighed.

Table DR1. Landslide input and suspended sediment discharge of sixteen gauging stations along the Longmen Shan.

Station	River	Area (km^2)	Runoff (mm yr^{-1})	Proportion >5 mm day^{-1} (%)	$Q_{ss\text{-}pre}$ (Mt yr^{-1})	$Q_{ss\text{-}post}$ (Mt yr^{-1})	Landslide area (km^2)	Landslide density (%)	Landslide input (Mt)	M_{fines} (Mt)	T_{fines} (yr)
Zhenjiangguan	Min J.	4,486	350±76	1.3	0.46±0.05	0.64±0.06	*	*	*	*	-
Heishui	Min J.	1,720	773±84	21.0	0.30±0.03	0.30±0.03	0.05	< 0.01	0.5+0.7/-0.3	0.03+0.05/-0.03	11+16/-10
Shaba	Min J.	7,231	543±81	5.4	1.55±0.16	0.77±0.08	0.23	< 0.01	2.1+2.0/-0.9	0.14+0.16/-0.11	-
Zagunao	Min J.	2,404	808±83	17.5	0.65±0.07	0.53±0.05	5.53	0.22	69+97/-40	5+7/-4	-
Sangping	Min J.	4,629	673±74	8.9	0.83±0.08	1.06±0.11	12.3	0.27	153+150/-63	10+12/-8	44+52/-34
Guojiaba	Min J.	555	663±184	48.7	0.10±0.01	0.57±0.06	9.71	1.71	84+101/-46	5+8/-5	12+16/-10
Dujiang	Min J.	22,947	349±32	0	0.39±0.04	2.12±0.21	163	0.71	2018+2529/-1039	133+189/-112	77+109/-65
Pingwu	Fu J.	4,310	764±121	13.7	1.38±0.14	2.60±0.26	5.02	0.12	85+147/-53	6+10/-5	5+9/-4
Jiangyou	Fu J.	5,915	515±93	17.2	1.59±0.16	2.27±0.23	8.37	0.14	125+158/-58	8+12/-7	12+17/-10
Ganxi	Fu J.	1,067	509±102	29.6	0.28±0.03	1.36±0.14	1.44	0.14	17+23/-10	1.1+1.7/-1.0	1.0+1.6/-0.9
Fujiangqiao	Fu J.	11,903	644±105	23.3	3.10±0.31	14.50±1.45	52.5	0.45	800+1282/-486	53+92/-48	5+8/-4
Zitong	Fu J.	1,547	512±196	66.0	0.27±0.03	0.73±0.07	*	*	*	*	-
Santai	Fu J.	2,343	442±114	33.2	0.07±0.01	0.47±0.05	20.2	0.79	1131+3056/-816	75+208/-73	190+528/-186
Pengshan	Min J.	30,661	372±82	8.9	1.09±0.11	4.14±0.41	172	0.56	2125+2534/-1040	140+192/-116	46+63/-38
Dengyingyan	Tuo J.	14,484	583±113	25.3	1.61±0.16	4.58±0.46	109	0.74	1789+2933/-1096	118+209/-107	40+70/-36
Shehong	Fu J.	23,574	480±87	25.0	1.46±0.15	9.78±0.98	109	0.47	2415+3386/-991	159+247/-125	19+30/-15
Total	-	68,719	478±126	-	4.56±0.46	18.50±1.85	390	0.57	6329+5097/-1787	418+437/-302	29+30/-21

*Negligible landslide coverage.

The runoff is based on the time period of 2006-2012 except Sangping station (2006-2011). $Q_{ss\text{-}pre}$ and $Q_{ss\text{-}post}$ are the average annual suspended sediment discharges before (2006-2007) and after (2008-2012) the earthquake, respectively. M_{fines} (Mt) is the estimated mass of landslide material with a grain size < 0.25 mm, which accounts for 4-9% of the total landslide mass. T_{fines} (yr) is the estimated time necessary for rivers to remove all M_{fines} based on the post-earthquake removal rates.

Table DR2. Uncertainty of suspended-sediment discharge at the Sangping station.

Year	*n*	Standard Deviation (%)	Standard Error (%)
2006	113	12.6	5.1
2007	112	12.3	5.8
2008	158	6.1	3.3
2009	117	8.1	4.6
total	500	10.1	4.9

n is the number of days with more than one SSC measurement. The standard deviation and standard error are reported as a percentage of the mean SSC.

Table DR3. Proportion of grains <0.25 mm from deposits of landslides triggered by the Wenchuan earthquake.

Site	Catchment	Weight % <0.25 mm	Reference
Xiaojiagou, Yingxiu S1	Min Jiang	3.0%	1
Xiaojiagou, Yingxiu S2	Min Jiang	6.0%	1
Xiaojiagou, Yingxiu S3	Min Jiang	3.0%	1
Xiaojiagou, Yingxiu S4	Min Jiang	3.0%	1
Xiaojiagou, Yingxiu S5	Min Jiang	3.0%	1
Xiaojiagou, Yingxiu S6	Min Jiang	3.0%	1
Xiaojiagou, Yingxiu S7	Min Jiang	3.0%	1
Xiaojiagou, Yingxiu S8	Min Jiang	5.0%	1
Niuquangou - a	Min Jiang	8.2%	2
Niuquangou - b	Min Jiang	7.0%	2
Niuquangou - c	Min Jiang	10.3%	2
Xiejiadianzi - a	Tuo Jiang	6.4%	2
Xiejiadianzi - b	Tuo Jiang	5.1%	2
Xiejiadianzi - c	Tuo Jiang	6.0%	2
Xiejiadianzi - d	Tuo Jiang	1.2%	2
Wenjiagou - a	Tuo Jiang	5.3%	2
Wenjiagou - b	Tuo Jiang	2.8%	2
Wenjiagou - c	Tuo Jiang	8.8%	2
Wenjiagou - d	Tuo Jiang	2.6%	2
Mianyuan River, p6	Tuo Jiang	3.8%	3
Mianyuan River, p9	Tuo Jiang	5.2%	3
Mianyuan River, p7	Tuo Jiang	7.4%	3
Mianyuan River, p11	Tuo Jiang	9.6%	3
Mianyuan River, p5	Tuo Jiang	10.8%	3
Mianyuan River, p10	Tuo Jiang	13.4%	3
Wenjiagou, site 1	Tuo Jiang	2.0%	4
Wenjiagou, site 2	Tuo Jiang	22.9%	4
Shiting River	Tuo Jiang	6.1%	5
Qingzhu River	Fu Jiang	4.3%	5
Weijiagou, site 1	Fu Jiang	6.1%	6
Weijiagou, site 2	Fu Jiang	6.7%	6
Weijiagou, site 3	Fu Jiang	8.7%	6
Weijiagou, site 4	Fu Jiang	16.8%	6
Average (n=33)		**6.6±4.4%**	

References: 1, Chen et al., 2012; 2, Wang et al., 2012; 3, Wang et al., 2013; 4, Yu et al., 2013; 5, Wang et al., 2011; 6, Zhuang et al., 2012.

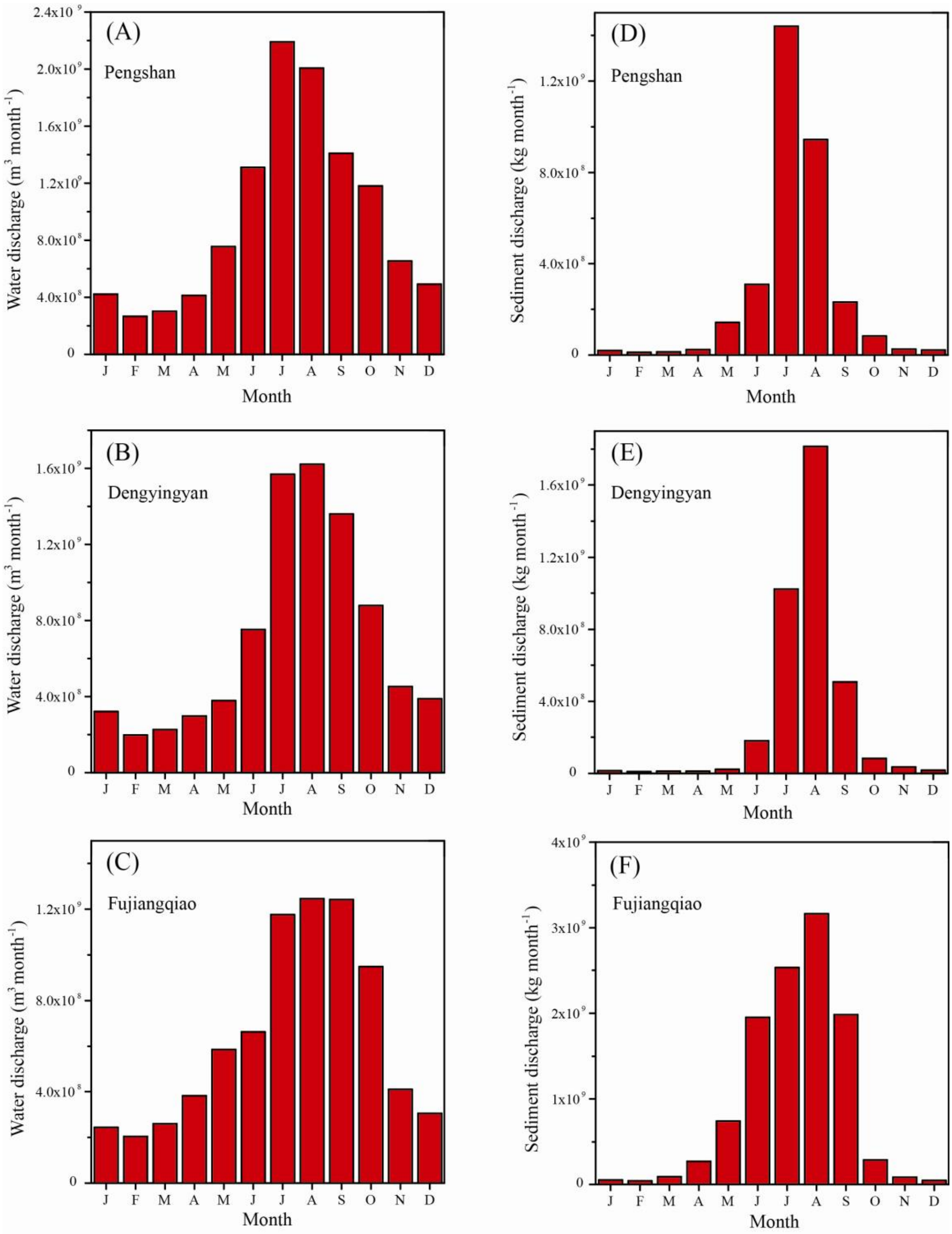

Figure DR1: Monthly variations of water discharge (m^3 $month^{-1}$) and suspended sediment discharge (kg $month^{-1}$) at three typical stations across the Longmen Shan from 2006 to 2012. (A and D) Pengshan station, (B and E) Dengyingyan station, and (C and F) Fujiangqiao station. Water discharge during April to October accounts for ~81% of total annual discharge, whereas suspended sediment discharge accounts for ~97% at these stations.

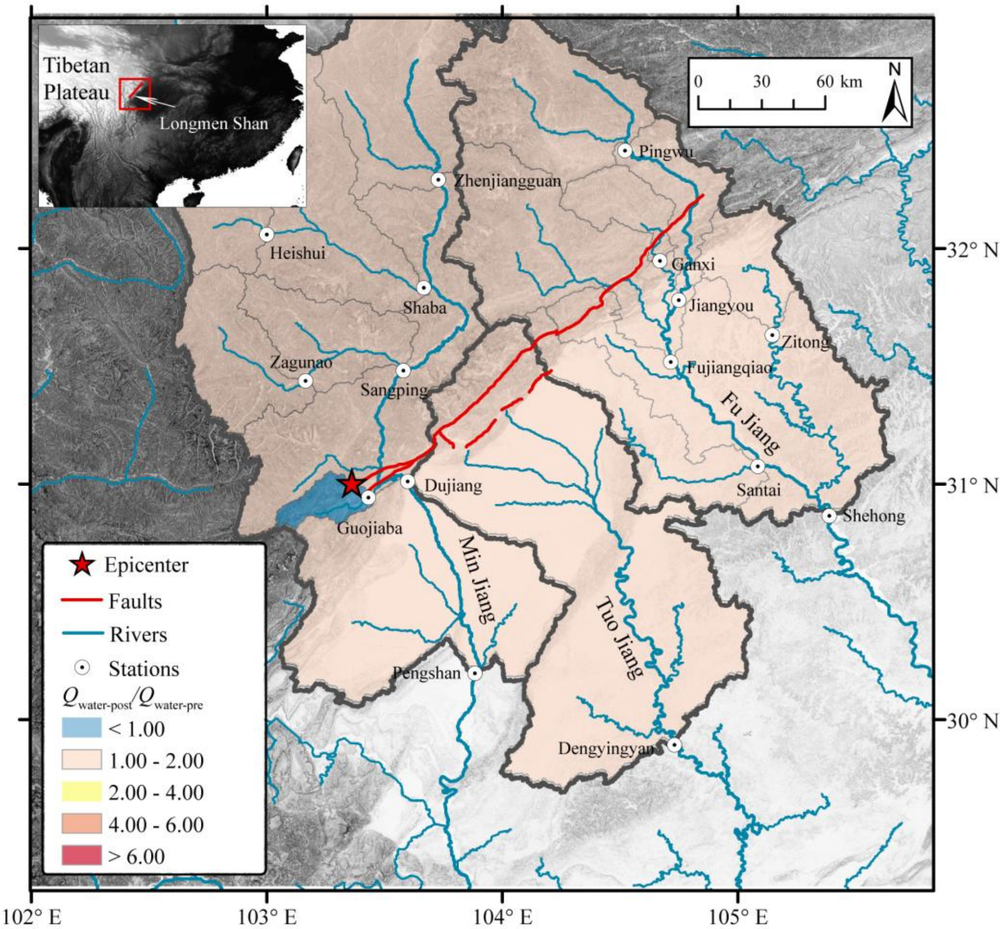

Figure DR2: Water discharge enhancement in rivers of the Longmen Shan following the Wenchuan earthquake. Catchment shadings reflect the ratios of mean annual water discharge (Q_{water}, m^3 yr^{-1}) after the Wenchuan earthquake to that prior to the earthquake for available gauging stations (circles). In order to compare with the ratios of suspended sediment enhancement in Fig. 1, we use the same class ranges for colour shadings. The large discrepancy between the water discharge enhancement (shown here) and the suspended sediment enhancement (Fig. 1) demonstrates that the changes of sediment load are not caused by variation in water discharge.

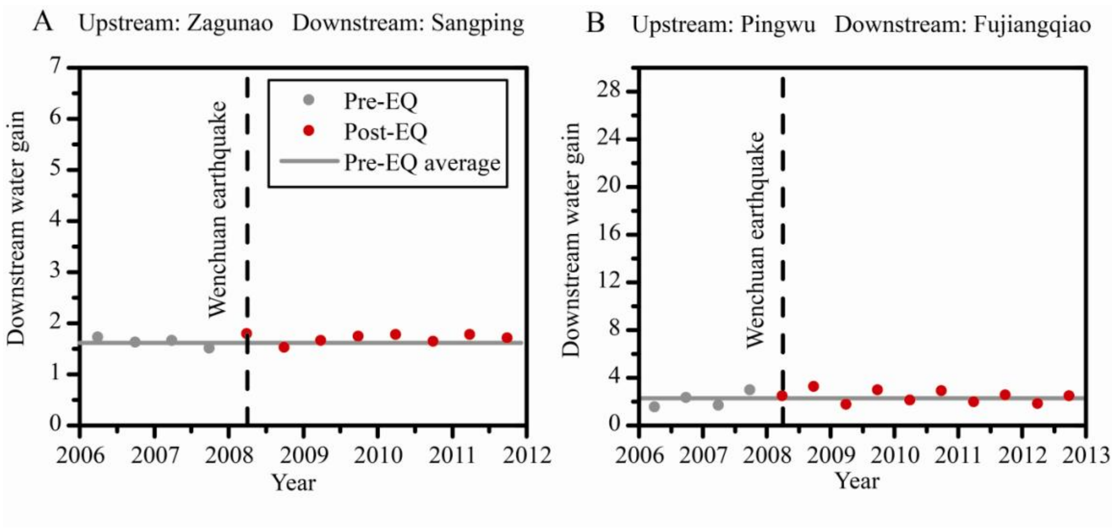

Figure DR3: A. Downstream water gain for nested gauging stations on the Zagunao River. B. Downstream water gain for nested gauging stations on the Fu Jiang. Downstream water gain is the ratio of downstream to upstream water discharge. In order to compare with the downstream sediment gain in Fig. 2B and 2C, we use the same ranges of axes.

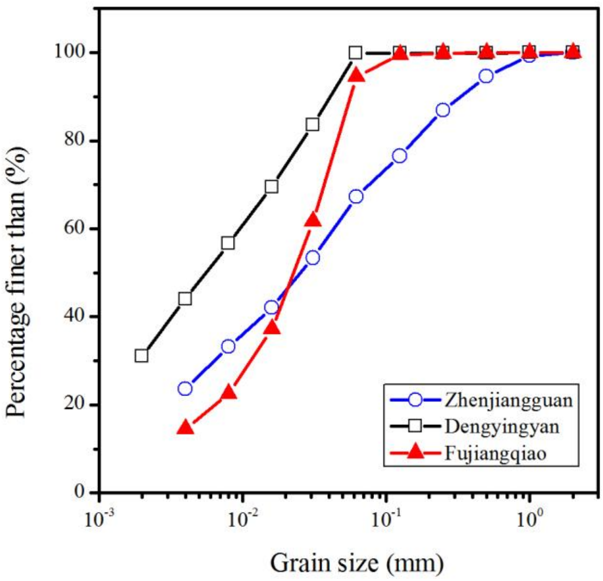

Figure DR4: Grain size distribution of suspended sediment in our studied rivers during 2007 to 2012. Over 95% of suspended sediment grain size is smaller than 0.25 mm. The blue line with open circles is grain size distribution of suspended sediment collected from Zhenjiangguan station on the Min Jiang; black line with squares is from Dengyingyan station on the Tuo Jiang; and the red line with triangles is from Fujiangqiao station on the Fu Jiang. The method for determining the grain size distribution followed the standard of the Ministry of Water Resources of China (2005).

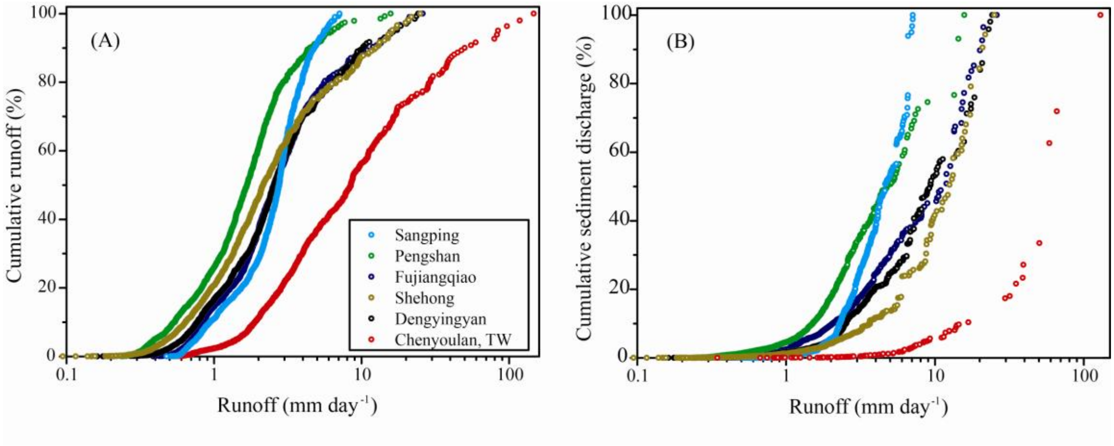

Figure DR5: The cumulative runoff (A) and sediment discharge (B) in Longmen Shan and in the Chenyoulan River, Taiwan after the Wenchuan and Chi-Chi earthquakes. Comparing to the rivers in the Longmen Shan, the Chenyoulan River has higher runoff, with higher frequency of high runoff events. Most of suspended sediment is mobilized during high runoff events.

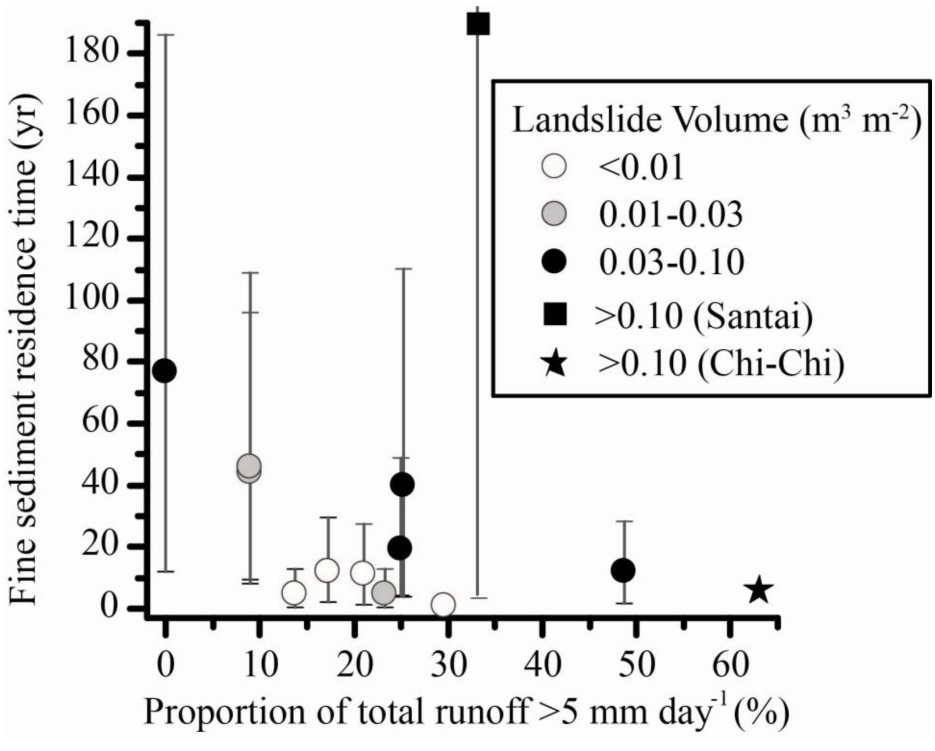

Figure DR6: Estimates of residence time of fine grained sediment mobilized by earthquake-triggered landslides in river catchments impacted by Wenchuan earthquake, plotted as a function of proportion of catchment intense runoff (>5 mm day^{-1}). Compared to Fig. 3, the symbols reflect the landslide volume per unit area caused by coseismic landslide. The residence time of Santai station (square, landslide density = 0.79%) is not well explained by the control of landslide density in Fig. 3. This is because there are some individual landslides with large volume, which contribute significant volumes of sediment, but this is not reflected in landslide area in this small (2,300 km^2) catchment.

References cited:

Chen, H.X., Zhang, L.M., Chang, D.S., and Zhang, S., 2012, Mechanisms and runout characteristics of the rainfall-triggered debris flow in Xiaojiagou in Sichuan Province, China: Natural Hazards, v. 62, p. 1037-1057, doi: 10.1007/s11069-012-0133-5.

Guy, H.P., 1969, Laboratory theory and methods for sediment analysis: U.S. Geological Survey Techniques of Water Resources Investigations, book 5, chap. C1, p. 23-28.

Ministry of Water Resources of China, 2005, Technical Standard for Determination of Sediment Particle Size in Open Channels (SL 42–2010): Beijing, China Water and Power Press (in Chinese).

Wang, G., Huang, R., Kamai, T., and Zhang, F., 2013, The internal structure of a rockslide dam induced by the 2008 Wenchuan (M_w7.9) earthquake, China: Engineering Geology, v. 156, p. 28-36, doi: 10.1016/j.enggeo.2013.01.004.

Wang, Y., Cheng, Q., and Zhu, Q., 2012, Inverse grading analysis of deposit from rock avalanches triggered by wenchuan earthquake: Chinese Journal of Rock Mechanics and Engineering, v. 31, p. 1089-1106 (in Chinese).

Wang, Z., Shi, W., and Liu, D., 2011, Continual erosion of bare rocks after the Wenchuan earthquake and control strategies: Journal of Asian Earth Sciences, v. 40, p. 915-925, doi: 10.1016/j.jseaes.2010.07.004.

Yu, B., Ma, Y., and Wu, Y., 2013, Case study of a giant debris flow in the Wenjia Gully, Sichuan Province, China: Natural Hazards, v. 65, p. 835-849, doi: 10.1007/s11069-012-0395-y.

Zhuang, J., You, Y., Chen, X., and Pei, L., 2012, Effect of infiltration and anti-scourability of mixed-grain-sized, unconsolidated soil on debris flow initiation: Bulletin of Soil and Water Conservation, v. 32, p. 43-47 (in Chinese).